Free Radical Research, September 2009; 43(9): 887–897

informa
healthcare

Free radical scavenging reactions and antioxidant activities of silybin: Mechanistic aspects and pulse radiolytic studies

HAIYING FU[1], MINGZHANG LIN[2], YUSA MUROYA[3], KUNIKI HATA[3], YOSUKE KATSUMURA[2,3,4], AKINARI YOKOYA[2], NAOYA SHIKAZONO[2], & YOSHIHIKO HATANO[2]

[1]*Radiation Chemistry and Technology Laboratory, Shanghai Institute of Applied Physics, Chinese Academy of Sciences, Shanghai 201800, PR China,* [2]*Advanced Science Research Center, Japan Atomic Energy Agency, 2-4 Shirakata shirane, Tokaimura, Nakagun, Ibaraki 319-1195, Japan,* [3]*Nuclear Professional School, School of Engineering, The University of Tokyo, 2-22 Shirakata shirane, Tokaimura, Nakagun, Ibaraki 319-1188, Japan, and* [4]*Department of Nuclear Engineering and Management, School of Engineering, The University of Tokyo, Hongo 7-3-1, Bunkyo-ku, Tokyo 113-8656, Japan*

(Received 25 March 2009; revised 23 June 2009)

Abstract

Silybin (extracted from *Silybum marianum*) is the major active constituent of silymarin which possesses a wide range of medicinal properties. These properties may be, in part, due to the potent scavenging capacity of oxidizing free radicals. In this context, scavenging radicals (hydroxyl, azide, dibromide anion radicals, nitrite, carbonate, etc.) of silybin have been studied to understand the mechanistic aspects of its action against free radicals. The transients produced in these reactions have been assigned and the rate constants have been measured by pulse radiolysis techniques. Reduction potential determined by cyclic voltammetry gave a value 0.62 ± 0.02 V vs NHE at pH 9. Quantum chemical calculations have been performed to further confirm the different activities of individual hydroxyl groups with the difference of heat of formation. Moreover, silybin also protected plasmid pUC18 DNA from soft X-ray radiation which induced strand breaks. These results are expected to be helpful for a better understanding of the anti-oxidative properties of silybin.

Keywords: *Silybin, free radicals, pulse radiolysis, antioxidant, kinetics and mechanism*

Introduction

In the last few decades, a substantial increase in the research pertaining to natural antioxidants has been observed due to their non-toxicity and interaction with various endogenous and exogenous free radicals in the living cells [1]. In spite of the comprehensive network of antioxidant defenses, many reactive oxygen species (ROS) still escape this surveillance and inflict various cytotoxic effects causing loss in structural/functional architecture of the cell. This oxidative damage leads directly to cytotoxicity and/or indirectly to genotoxicity with numerous serious anomalies favouring disharmony and diseases [2].

The interest in antioxidants related to food and herbal medicine is getting popularized due to their natural origin, cost effectiveness, no side effects and multifaceted activities. These provide enormous scope in correcting the oxidative imbalance, serving humans as food components, seasonings, beverages, cosmetics as well as medicine. The World Health Organization has estimated that $\sim$ 80% of the earth's inhabitants rely on traditional medicine for their primary health care needs and most of these therapies involve the use of preparations from plant extracts [3]. Some of the popular formulations used as drugs for liver diseases and GIT (gastrointestinal tract) problems consist of parts of a plant, *Silybum marianum* [4].

Correspondence: Dr Haiying Fu, Radiation Chemistry and Technology Laboratory, Shanghai Institute of Applied Physics, Shanghai, 201800, PR China. Email: tf.erine2008@gmail.com; or Prof. Dr Katsumura, Department of Nuclear Engineering and Management, School of Engineering, the University of Tokyo, Hongo 7-3-1, Bunkyo-ku, Tokyo 113-8656, Japan.

ISSN 1071-5762 print/ISSN 1029-2470 online
DOI: 10.1080/10715760903136996

Silybin(3,5,7-trihydroxy-2-[9-(4-hydroxy-3-methoxy-phenyl)-8-(hydroxymethyl)-7,10-dioxabicyclo[4.4.0]deca-2,4,11-trien-3-yl]chroman-4-one) (Figure 1), isolated mainly from the seeds of milk thistle (namely *Silybum marianum*), is an active component in a number of phytopreparations, for example, flavobin™ and legalon™. The flavonoid structure of silybin makes it easy to form an intramolecular hydrogen bond [5]. Silybin is widely used in the treatment and prevention of chronic inflammatory 1iver disorders, diseases caused by γ-radiation and toxic chemicals such as carbon tetrachloride, galactosamine, thioacetamide, ethanol, benzo[a]pyrene, thallium, α-amanitin, etc [6,7]. It functions as a free radical scavenger of active and stable oxygen radicals. Growing interest in new activities of silybin in non-traditional applications is documented by the fact that $\sim$800 new papers on this topic have been published in the last 5 years [8].

So far, the studies on silybin were focused on its pharmacological characteristics and clinical effects, the molecular mechanisms of the antioxidative activity of silybin have not been systematically investigated and remain unclear. The poor solubility of silybin in water at neutral pH limited the chemical kinetics studies to a certain degree. Therefore, instead of pure silybin, the glycosides of silybin such as dihemisuccinate salt were used to study the one electron oxidation by pulse radiolysis in the 1990s [9,10]. In one of our previous studies, laser flash photolysis was carried out in its alcoholic solutions [11].

This paper aims to explain the markedly high antioxidant activity of silybin at the molecular level. In order to understand the ability to react with the free radicals and the mechanism underlying the free radical reactions, nanosecond pulse radiolysis techniques were employed and the reaction of hydroxyl, azide and other oxidizing radicals with silybin have also been studied in detail. And the reduction potential of silybin was determined by the cyclic voltammetry method. Moreover, silybin also protected pUC 18 plasmid DNA from soft X-ray-induced strand breaks as evidenced from studies on agarose gel electrophoresis of the plasmid DNA after radiation exposure. For the quantum chemical calculations, a semi-empirical AM1 study has been performed to optimize the structure of parent compound and the radicals generated by H-abstraction reactions from individual hydroxyl groups. Bond dissociation energies have further been calculated using a hybrid density functional theory (DFT) at B3LYP level for the respective H atom elimination paths.

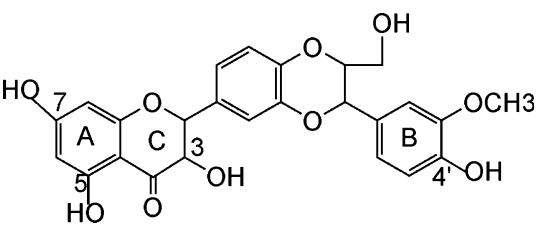

Figure 1. The chemical structure of silybin.

Materials and methods

Materials

Silybin (SLB), naringin, ethidium bromide were purchased from Sigma (Sigma-Aldrich, Japan) and used as received. Perchloric acid was GR products, phosphate buffer and sodium hydroxide were of analytical grade, and the other reagents were of the highest purity. They were purchased from Wako Pure Chemical Industries, Ltd. (Japan). Water was purified through a Millipore system (Milli-Q, Element A-10). Unless otherwise indicated, all solutions were freshly prepared before each experiment. Sample solutions were bubbled with high purity argon, nitrous oxide or oxygen for each purpose over 20 min. All experiments were carried out at room temperature.

Reactions with oxidizing species

Free radicals were generated by using standard methods for converting primary species of the radiolysis of water, e_{aq}^-, $^\bullet OH$ and $^\bullet H$. When the sample solution was saturated with N_2O for 20 min prior to pulse radiolysis, e_{aq}^- was scavenged to form OH radical. The yield of OH radical under such conditions was 90% of the total [$G(^\bullet OH) = 5.5$ molecule/100 eV $= 5.7 \times 10^{-7}$ mol/J]. The remaining 10% contribution came from that of $H^\bullet$-atoms [$G(^\bullet H) =$ 0.55 molecule/100 eV $= 0.57 \times 10^{-7}$ mol/J].

$$H_2O \rightsquigarrow {}^\bullet OH,\ e_{aq}^-,\ H^\bullet,\ H_2O_2,\ HO_2 \quad (1)$$

$$e_{aq}^- + N_2O + H_2O \rightarrow {}^\bullet OH + OH^- + N_2$$
$$k_2 = 9.0 \times 10^9\ dm^3/mol/s\ [12] \quad (2)$$

In order to quantitatively generate secondary electron oxidants, $N_3^\bullet$ and $Br_2^{\bullet -}$, the following well-known OH radical reactions (3–4) were used. Subsequent reaction of these secondary oxidants with silybin resulted in the generation of one-electron oxidized silybin species.

$$^\bullet OH + N_3^- \rightarrow N_3^\bullet + OH^- \quad (3)$$

$$^\bullet OH + Br^- \rightarrow Br^\bullet + OH^- \quad (4a)$$

$$Br^- + Br^\bullet \rightarrow Br_2^{\bullet -} \quad (4b)$$

$$^\bullet OH + NO_2^- \rightarrow NO_2^\bullet + OH^-$$
$$k_5 = 1.0 \times 10^{10}\ dm^3/mol/s\ [13] \quad (5)$$

$$^\bullet OH + CO_3^{2-} \rightarrow CO_3^{\bullet -} + OH^-$$
$$k_6 = 3.9 \times 10^8\ dm^3/mol/s \quad (6)$$

Trichloroperoxyl radicals were generated according to the method of Gyorgy et al. [10], by delivery of an electron pulse to an O_2-saturated aqueous solution

containing 48% *iso*-propanol and 4% CCl_4 when following reactions (7–11) take place.

$$^{\bullet}OH + (CH_3)_2CHOH \rightarrow (CH_3)_2{}^{\bullet}COH + H_2O \quad k_7 = 1.9 \times 10^9\ dm^3/mol/s \tag{7}$$

$$H^{\bullet} + (CH_3)_2CHOH \rightarrow (CH_3)_2{}^{\bullet}COH + H_2 \quad k_8 = 7.4 \times 10^7\ dm^3/mol/s \tag{8}$$

$$(CH_3)_2{}^{\bullet}COH + CCl_4 \rightarrow {}^{\bullet}CCl_3 + (CH_3)_2CO + H^+ + Cl^- \quad k_9 = 7.0 \times 10^8\ dm^3/mol/s \tag{9}$$

$$e_{aq}^- + CCl_4 \rightarrow CCl_4^-{}^* \rightarrow {}^{\bullet}CCl_3 + Cl^- \quad k_{10} = 3.0 \times 10^{10}\ dm^3/mol/s \tag{10}$$

$$^{\bullet}CCl_3 + O_2 \rightarrow Cl_3COO^{\bullet} \quad k^{11} = 3.3 \times 10^9\ dm^3/mol/s\ [14, 15] \tag{11}$$

In neutral pH, Ar-bubbled aqueous solution containing *t*-BuOH as an OH radical scavenger reaction (12) takes place. G $(e_{aq}^-) = 2.75$ molec/100 eV $= 2.8 \times 10^{-7}$ mol/J.

$$^{\bullet}OH + (CH_3)_3COH \rightarrow H_2O + {}^{\bullet}CH_2(CH_3)_2COH \quad k^{12} = 6.6 \times 10^9\ dm^3/mol/s\ [16] \tag{12}$$

In the system, $^{\bullet}H$ and e_{aq}^- react with $S_2O_8^{2-}$ to produce $SO_4^{\bullet -}$ (equations 13 and 14).

$$SO_4^{\bullet -} + SO_4^{2-} \rightarrow SO_4^{\bullet} + SO_4^{2-} \tag{13}$$

$$^{\bullet}H + S_2O_8^{2-} \rightarrow SO_4^{\bullet -} + HSO_4^- \tag{14}$$

Pulse radiolysis

Pulse radiolysis method is a popular technique to observe the interaction of chemicals and free radicals. In the present work, the 35 MeV LINAC accelerator at the University of Tokyo provided 10 ns pulse width electron beam using an absorption spectrometric system and the dosimetry was based on the initial yield of dithiocyanate radical anion obtained in N_2O-saturated samples of 10^{-2} mol/dm^3 KSCN aqueous solution ($G \times \varepsilon = 5.1 \times 10^4$ m^2/J) at 472 nm [17]. Detailed descriptions of the set-up of pulse radiolysis equipment and experimental conditions have been described elsewhere [18]. In the present work, the absorbed dose was usually $\sim$15 Gy/pulse for studying the reaction kinetics with the substrate. A higher dose of $\sim$65 Gy/pulse was used to record the absorption spectra. The sample solution was kept flowing through the quartz cell and was changed completely after each electron-beam pulse by a Teflon pump. The optical length of the quartz cell was 1.8 cm. Because of the poor solubility of silybin in neutral aqueous solutions, the samples were first dissolved in alkaline solutions, then adjusted to neutral pH using $HClO_4$.

Cyclic voltammetry

Cyclic voltammetry studies were carried out on an Autolab Electrochemical System equipped with PGSTAT 20 and driven by GPES software. The working electrode was a highly polished glassy carbon electrode (GCE) with a diameter of 2 mm, and a platinum wire was used as a counter electrode. The reference electrode was saturated calomel reference electrode (SCE) with a salt bridge containing 3.0 mol dm^{-3} KCl aqueous solutions. The GCE surface was polished with aqueous slurry of alumina powder before each measurement. The solution pH was adjusted by adding dilute acid/alkali. Solutions were de-aerated by bubbling N_2 for 10 min prior to recording the cyclic voltammogram. The observed potential values were against SCE and converted to those vs the normal hydrogen electrode (NHE) by adding 0.24 V to the observed values.

Estimation of DNA damage

Radiation-induced damage in DNA was determined by the conversion of supercoiled pUC 18 plasmid DNA to open circular (*oc*) and linear forms, according to the procedure described previously [19]. Immediately after irradiation, the different forms of DNA were separated by agarose gel electrophoresis. Briefly, the mixture contained 150 ng plasmid pUC18 in 2.0×10^{-2} mol/dm^3 phosphate buffer, pH 7.4, in the presence or absence of 2.5×10^{-5} dm^3 silybin. After soft X-ray irradiation at 50 Gy, the DNA samples were applied to 1% agarose gels in $0.5 \times$ TBE buffer consisting of 8.9×10^{-2} mol/dm^3 Tris Borate/2.0×10^{-3} mol/dm^3 EDTA, pH 8.3 [20], and electrophoresis was performed at 140 V for 315 min. The gels were stained with ethidium bromide and DNA bands were photographed and analysed. The modification of the fluorescence intensity of the bands is due to DNA band breakage that leads to a decrease in the proportion of supercoiled form (*sc*) and to an increase in linear form and open circular DNA. The relative amount of DNA in each form was then estimated by integration of the intensity of the pixels comprising each band. Relative to the open-circular and linear conformations, intensities of supercoiled bands was multiplied by a factor of 1.4 to account for the lower binding constant for ethidium to supercoiled plasmid, as discussed previously [21]. The percentage of *sc* form remaining of DNA was used to estimate the degree of radiation-induced DNA damage [22].

Calculation of the G value for single-strand breaks (SSB) formation

DNA single-strand breaks (conversion of supercoiled to open circle) following irradiation in the presence or absence of added silybin was determined in 2.0×10^{-2} mol/dm^3 phosphate buffer solution. A dose response was determined from the logarithmic loss of supercoiled plasmid DNA on radiation dose. Plotting the logarithm of the fraction of survival supercoiled

DNA against radiation dose gave a straight line (Figure 7B). The parameter of dose response D_0 was calculated from the reciprocal of the slope of the straight line, according to the equation below [23]:

$$D_0 = [(\log_{10}37) - 2]/\text{slope}$$

At D_0, the concentration of single strand breaks (SSB) is equal to the concentration of DNA expressed as plasmid molecules (relative molecular mass = 650 g/mol/bp × number of base pair). From the definition of the G value (in units of μmol/J), the G value for SSB formation, G(SSB) is equal to (DNA concentration/μmol/dm^3)/[(D_0/Gy) × (ρ/kg/dm^3)]. The density of the solution, ρ, is assumed to be unity as previously described [24]. At least six points were used in the estimation of each D_0. Usually the highest dose applied was two or three times of D_0.

Quantum chemical calculations

Ab initio molecular orbital techniques have been used to investigate the structure and energetics of silybin and possible radical species (obtained by H-atom abstraction from it). The bond dissociation energy (BDE) of O-H was calculated as the difference in total enthalpy between the silybin phenoxyl radical (SLB-PhO$^\bullet$) formed after H abstraction and silybin (SLB-PhOH), according to the following reaction: SLB-PhOH → SLB-PhO$^\bullet$ + H$^\bullet$.

As the size of silybin is generally big, contains 57 atoms, the *ab initio* method is obviously difficult to be used for mechanistic computation of reaction between silybin and radicals. Thus, the semi-empirical method AM1 [25] was employed to perform a complete geometry optimization. The geometry optimization of each ArO$^\bullet$ radical was performed starting from the optimized structure of the parent molecule, after the H atom was removed from the 3, 5, 7 or 4′ position. Calculations were carried out without taking into account the solvent effects. Guerra et al. [26] studied the effect of explicit water molecules on phenol. They concluded that solvent molecules could be arranged in cages (of at least six water molecules) in the vicinity of the OH group of phenol. Such calculations for each OH group of silybin would have been untraceable. The detailed calculation procedures are as follows. The molecular geometries were optimized by semi-empirical quantum chemical method AM1 and then by DFT method B3LYP/6-31G (d) functional on basis set of 6-31G(d) to calculate single point energy (SPE). All of the calculations were performed using Gaussian-03W program package [27].

Results and discussion

Reactions with $N_3^\bullet$ or $Br_2^{\bullet-}$ radical

$N_3^\bullet$, as well as $Br_2^{\bullet-}$ radicals, are moderately strong one-electron oxidants that can oxidize phenols and polyphenols [28]. These radicals are conveniently generated by the reaction of bromide or azide ions with OH radicals, formed in the radiolysis of water (reactions 1–4).

Pulse radiolysis of N_2O-saturated aqueous solution containing 1×10^{-3} mol/dm^3 silybin and 0.05 mol/dm^3 NaN_3 or KBr at pH 7.8, led to the initial formation of $N_3^\bullet$ or $Br_2^{\bullet-}$, respectively, which subsequently oxidized silybin *via* electron transfer reaction. The transient spectrum obtained after the reaction of $N_3^\bullet$ with silybin was shown in Figure 2 with a narrow maximum absorption peak at 370 nm and the other broad absorption band from 480–600 nm, which is similar to that obtained from reaction of $Br_2^{\bullet-}$ with silybin (data were not shown). While the band at 580 nm decayed within 10 μs, only a slight formation at 370 nm on this time scale was observed (Figure 2, inset). The difference of kinetic behaviours at 370 and 580 nm suggests the formation of at least two types of transient species, which is in good agreement with the literature [10]. The assignment of the species will be discussed in detail later.

Due to the strong absorption of silybin aqueous solution below 380 nm, second-order rate constants for reactions with $N_3^\bullet$ were derived from the build-up of phenoxyl radicals at 580 nm. By varying the five silybin concentrations between 2×10^{-4} to 1.0×10^{-3} mol/dm^3, we derived the rate constants, $(2.0 \pm 0.2) \times 10^9$ dm^3 mol^{-1} s^{-1}. With increasing the pH to 11, the rate constants increased to 5.7×10^9 dm^3/mol/s. Such an increase is due to the existence of an acid-base equilibrium. Similar phenomena have

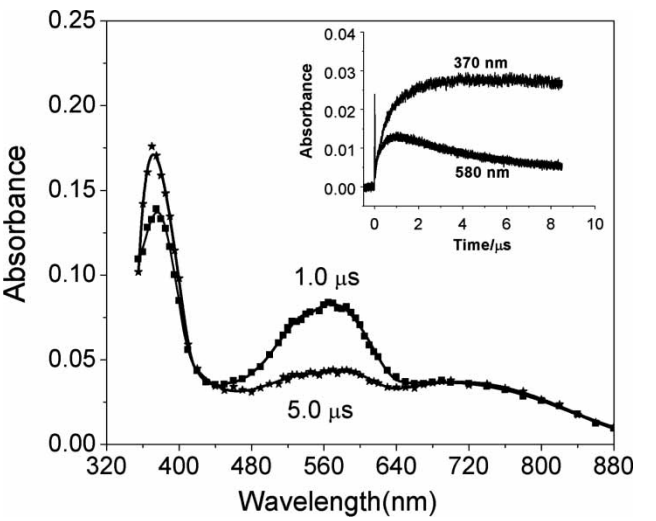

Figure 2. Transient absorption spectra from pulse radiolysis of 1.0×10^{-3} mol/dm^3 silybin and 0.05 mol/dm^3 NaN_3 aqueous solution saturated with N_2O at pH 7.8, recorded at 1.0 and 5.0 μs after pulse. Inset: the buildup trace of absorption at 370 and 580 nm.

been reported by Gyorgy et al. [10], in the case of pulse radiolysis of 2-hydroxy-4-(3-sulpho-1-propyloxy)-acetophenone. They attributed the pH effect to the chelatic H-bonding interaction between the oxo and the OH groups at low pH.

The transient absorption spectrum formed by $Br_2^{\bullet -}$ reacting with silybin was similar to that by $N_3^{\bullet}$ radical. The formation rate constant was estimated to be $(3.9 \pm 0.2) \times 10^8$ dm^3/mol/s. Since $N_3^{\bullet}$ and $Br_2^{\bullet -}$ are considered to be moderate oxidants, the easy oxidation of silybin by $N_3^{\bullet}$ or $Br_2^{\bullet -}$ might imply a strong antioxidative ability of silybin.

Reaction with OH radical

Among the various ROS, OH radical is the most reactive oxidant and is the most predominant ROS generated endogenously during aerobic metabolism. Effective scavenging of this radical is important from the health perspective.

An aqueous N_2O-saturated solution of 1.0×10^{-3} mol/dm^3 silybin at pH 8.5 was pulse-irradiated. The spectrum was uncorrected for a small contribution ($\sim$10%) due to the H-atom reaction with the substrate. Both a strong and narrow absorption band in the 370 $\sim$ 390 nm range and the other quite broad absorption band in the 480 $\sim$ 640 nm range were similar to that observed during $N_3^{\bullet}$ or $Br_2^{\bullet -}$ radical reacting with silybin (Figure 3). Overall rate coefficients for OH radicals were determined by competition kinetics, using the formation of $(SCN)_2^{\bullet -}$ as the reference reaction, with k(OH + SCN^-) = 1.1×10^{10} dm^3/mol/s. Rate constants for the reactions of free radicals with the substrates are summarized in Table I. Silybin reacts with $^{\bullet}$OH and, at alkaline pH, azide radicals at a diffusion-controlled rate. The values are in good consistent with the

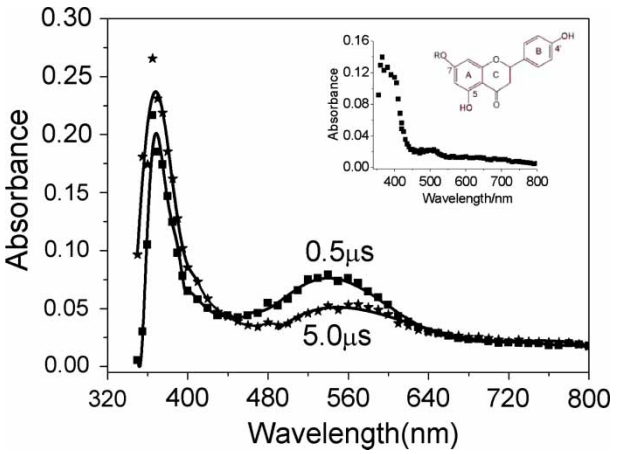

Figure 3. Transient absorption spectra from pulse radiolysis of 1.0×10^{-3} mol/dm^3 silybin aqueous solution at pH 8.5 purged with N_2O. Inset: Transient absorption spectra of naringin (R was substituted by Rhamnoglucoside at Ring A, C-7), at 1.0 μs after pulse.

Table I. Kinetic and spectroscopic properties for the reaction of oxidizing radicals with silybin in aqueous solution.

Radical	pH	λ_{max}/nm	$k \times 10^{-9}$ (dm^3/mol/s)
$^{\bullet}$OH	8.0		18
$N_3^{\bullet}$	7.8	580	2.0
$N_3^{\bullet}$	11	580	5.7
$Br_2^{\bullet -}$	7.8	370	0.39
$SO_4^{\bullet -}$	8.5	520	1.2
$NO_2^{\bullet}$	7.8	390	0.083
$CO_3^{\bullet -}$	11	380	0.19
$CCl_3OO^{\bullet}$	11	380	0.035
dGMP	7.0	370	1.0 [48]

results obtained from silybin dihemisuccinate-Na salt [10].

By analogy with the spectra shown in Figure 3 inset, the glucoside substituted of naringin at ring A C-7 caused no absorption band around 520–600 nm. Moreover, according to the literature [10], the absorption band appearing in the 480–600 nm is attributed to the 7- O$^{\bullet}$ phenoxyl radical, the other is assigned to the 4′- O$^{\bullet}$-methoxy-phenoxyl radical. Hydroxyl radicals are known to form adduct with aromatic rings. The decay of OH- adducts to phenoxyl radical around 315 nm was not observed due to strong absorption from the ground state. Even though at pH 11 $\sim$17% of hydroxyl radicals exist in the deprotonated form (O$^{\bullet -}$) and may react in different way, there was no significant change in the transient absorption spectra around pH 11 and 8.

As compared to the reaction with the azide radicals, in this case, the transient absorbencies were a little lower. This may be explained as follows. The azide radicals can react with silybin via only the pathway of H-atom abstraction or electron transfer, which leads to the formation of phenoxyl radical. However, the hydroxyl radical can also undergo the pathway of addition to form OH-adducts. Possibly, besides one electron oxidation, the hydroxyl radicals also form an addition with silybin, leading to a little lowering in the phenoxyl radical concentration. Moreover, the transient absorbances due to the adduct formation might have a lower absorption coefficient below 350 nm. Both of these factors contribute to the bleaching signal at the 300–350 nm (Figure 3) wavelength regions.

Reaction with $SO_4^{\bullet -}$ radicals

$SO_4^{\bullet -}$ radical was also used as one-electron oxidant in many studies. On the pulse radiolysis of aqueous solution containing 1.0×10^{-3} mol/dm^3 silybin, 0.02 mol/dm^3 $K_2S_2O_8$, 0.1 mol/dm^3 *t*-BuOH and saturated with argon, a transient optical absorption spectrum appeared and was characterized by a maximum absorption at 460 nm after 50 ns.

In the case of silybin, accompanying the absorption decay of $SO_4^{\bullet -}$ radical, the radical cation of silybin

with absorption peak at 370 nm and a broad absorption region from 500–560 nm appeared subsequently (Figure 4).

Then, $SO_4^{\bullet -}$ reacts with silybin to form phenoxyl radicals ($PhO^{\bullet}$) (equation 15):

$$SLB + SO_4^{\bullet -} \rightarrow SLB\text{-}PhO^{\bullet} + SO_4^{2-} + H^+ \quad (15)$$

The kinetics at $\lambda = 520$ nm contains not only the formation of silybin phenoxyl radical, but also the decay of $SO_4^{\bullet -}$. Due to the overlap of an absorption at 520 nm, we roughly separated the formation of silybin phenoxyl radical by subtracting the time profile at 460 nm (multiplied by a factor of A_{520}/A_{460}) from that at 520 nm, following the method reported by Jian et al. [29] The calculated time profile, trace c, as shown in the inset of Figure 4, is synchronous with the decay of $SO_4^{\bullet -}$ radical at 460 nm. From kinetic analysis of the growth trace at 520 nm, the reaction rate constants of silybin with $SO_4^{\bullet -}$ was calculated to be $(1.2 \pm 0.1) \times 10^9$ dm^3/mol/s.

Reaction with $CO_3^{\bullet -}$ and $NO_2^{\bullet}$ radical

Nitrogen dioxide radical ($NO_2^{\bullet}$) and carbonate radical ($CO_3^{\bullet -}$) are two well-known toxic species and strongly oxidizing radicals. Their one-electron redox potentials in neutral aqueous solution are $E(NO_2^{\bullet}/NO_2^-) = 1.0$ V and $E(CO_3^{\bullet -}/CO_3^{2-}) = 1.59$ V [30,31], respectively. In particular, the $NO_2^{\bullet}$ radical could be found in the cigarette smoke, car exhausts and chimney smoke from the factories [32]. As a common atmospheric pollutant, the $NO_2^{\bullet}$ radical is believed to be related to the development of oral/lung cancers and heart disease in smokers [33]. In biological systems, several modes of deleterious actions of $NO_2^{\bullet}$ and $CO_3^{\bullet -}$ have been proposed. Moreover, both $NO_2^{\bullet}$ and $CO_3^{\bullet -}$ have been demonstrated to selectively oxidize tyrosine and cysteine residues in peptides [34], leading to the loss of activity of enzymes. To gain further insight into the antioxidant activity of silybin, the reactions of $NO_2^{\bullet}$ and $CO_3^{\bullet -}$ with silybin were studied by pulse radiolysis technique.

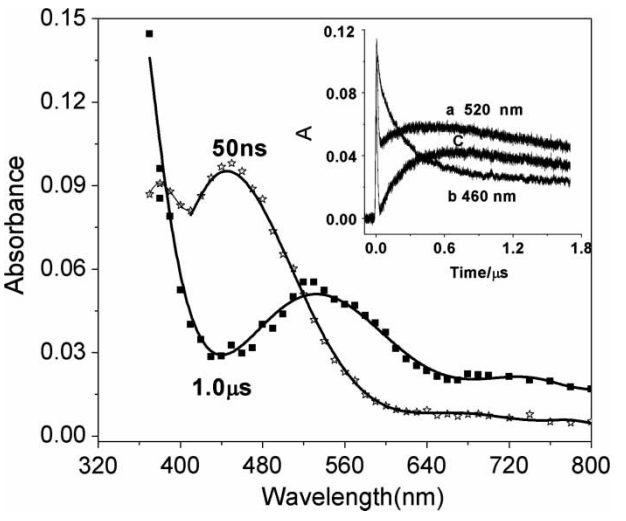

Figure 4. (A) Transient absorption of the species formed during pulse radiolysis of silybin aqueous solution (1.0×10^{-3} mol/dm^3) containing 0.1 mol/dm^3 tert-butanol, 0.02 mol/dm^3 $K_2S_2O_8$ and degased with argon at pH 8.5 (dose 65 Gy). (B) Inset: (a) time profile at 520 nm, (b) the decay at 460 nm, (c) absorbance obtained by subtracting trace (b) multiplied by A_{520}/A_{460} from trace a [29].

By pulse radiolysis 5.0×10^{-2} mol/dm^3 nitrite anion, 10^{-3} mol/dm^3 silybin, N_2O-saturated at pH 7, $NO_2^{\bullet}$ radicals were initially formed via reactions (2) and (5). The rate constant was obtained to be $(8.3 \pm 0.3) \times 10^7$ dm^3/mol/s.

Generation of $CO_3^{\bullet -}$ radicals was carried out by pulse radiolysis of a N_2O saturated aqueous solution containing 5.0×10^{-2} mol/dm^3 sodium carbonate and 1×10^{-3} mol/dm^3 silybin at pH 11. The rate constant was obtained to be $(1.9 \pm 0.2) \times 10^8$ dm^3/mol/s.

Comparing the reaction rate constants of $NO_2^{\bullet}$ with bio-molecules, such as tyrosine (3.2×10^5 dm^3/mol/s), glycyltyrosine ($< 1 \times 10^5$ dm^3/mol/s) [35], and the reaction rate constants of $CO_3^{\bullet -}$ with tyrosine (4.5×10^7 dm^3/mol/s), the reaction rate constants of silybin with $NO_2^{\bullet}$ or $CO_3^{\bullet -}$ are $(8.3 \pm 0.4) \times 10^7$ and $(1.9 \pm 0.2) \times 10^8$ dm^3/mol/s, respectively, which are much higher. Therefore, silybin is an efficient scavenger of $NO_2^{\bullet}$ and $CO_3^{\bullet -}$ radicals, which is expected to protect the cell membrane and enzymes against oxidation by $NO_2^{\bullet}$ and $CO_3^{\bullet -}$.

Reaction with trichloromethyl-peroxyl radical

CCl_4 is a known hepato-toxic chemical whose toxic action is due to its metabolism to an activated free radical of the type $CCl_3OO^{\bullet}$. $CCl_3OO^{\bullet}$ is capable of inducing lipid peroxidation [36]. This radical in particular has been widely used as a model compound for studying its reactivity with organic substrates, primarily because the haloperoxyl radicals are known to possess higher reactivity as compared to their unhalogenated analogues, due to the electron withdrawing nature of the halide ions.

It is very convenient to use $CCl_3OO^{\bullet}$ as a peroxyl radical model because it can be generated in water/alcohol solution, in which sufficient solubility of the substrate can be obtained. Figure 5 shows the transient absorption spectra after pulse radiolysis of alkaline solvent containing 1.0×10^{-3} mol/dm^3 silybin saturated with O_2. A new absorption band appears around 380 nm. Since the absorption peak of $CCl_3OO^{\bullet}$ is located at $\lambda < 320$ nm [37], the absorption band around 380 nm should be assigned to the phenoxyl radical of silybin arising from electron transfer reaction between $CCl_3OO^{\bullet}$ and silybin. After capture of one electron, $CCl_3OO^{\bullet}$ was deduced to CCl_3OO^- at pH 11.

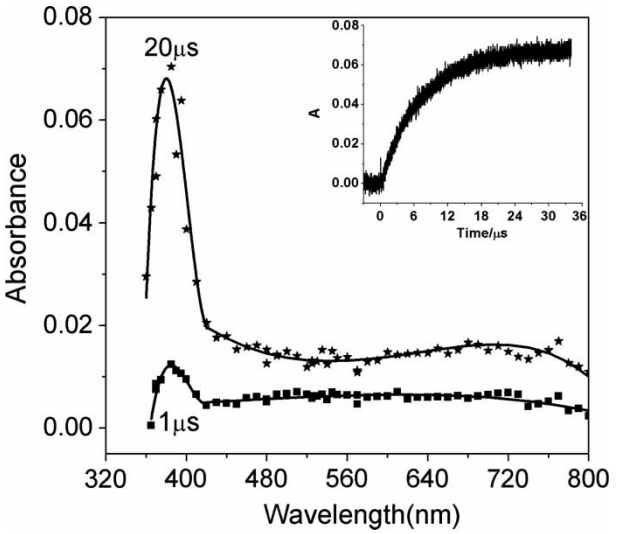

Figure 5. Transient absorption spectra from pulse radiolysis of silybin alkaline solvent (1.0×10^{-3} mol/dm^3) saturated with O_2 at pH 11 (dose 65 Gy). Inset: Growth trace of the transient absorption of the phenoxyl radical of silybin at 380 nm.

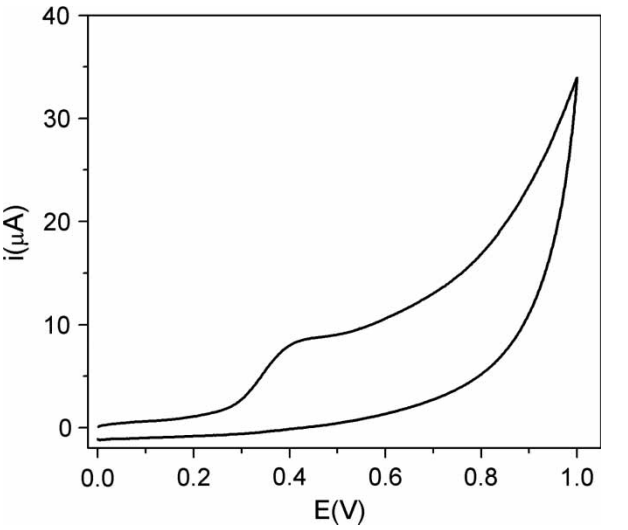

Figure 6. Cyclic voltammogram obtained for 2.0×10^{-3} mol/dm^3 silybin in N_2-bubbled aqueous solutions containing 0.1 mol/dm^3 KCl, 5.0×10^{-3} mol/dm^3 phosphate buffer, pH 9, and at a scan rate of 50 mV/s.

$$CCl_3OO^{\bullet} + SLB^{\bullet +} \rightarrow CCl_3OO^{-} + SLB^{\bullet} \qquad (16)$$

The buildup trace of the phenoxyl radical of silybin at 380 nm is shown as Figure 5 inset. It follows well the pseudo-first-order rate law. By varying silybin concentration ($0.4–1.0 \times 10^{-3}$ mol/dm^3) at pH 11, the rate constant for electron transfer from silybin to $CCl_3OO^{\bullet}$ was determined as $(3.5 \pm 0.2) \times 10^7$ dm^3/mol/s.

Reduction potential of silybin

Cyclic voltammetry has been often used to determine the redox potential and the total antioxidant capacity of natural products, biological samples, etc. [38]. Since silybin is present in many health foods, it is quite pertinent to determine its reduction potential in aqueous medium. The voltammograms were run for aqueous silybin solutions at pH 9 employing scan rates of 50 mV/s. Only one anodic peak was observed in the forward scan (Figure 6), whereas no peak was observed during the reverse scan indicating that the oxidation products were unstable or undergo electrode reaction or due to fast second order decay of radicals. From the anodic peak observed at 0.38 V, the reduction potential of silybin for the couple of the type (ArO$^{\bullet}$/ArOH) was 0.62 ± 0.02 V vs NHE at pH 9. This value is comparable (or in good agreement) with the reported one, 0.62 V, where 4-methoxyphenol was used as reference at pH 7 [10], while the reduction potential was related to pH value. For example, 542–572 mV to pH 7 [39], 400 mV to pH 13.5 [10].

Protection of plasmid pUC18 DNA damaged by soft X-ray

Exposure of plasmid pUC18 DNA to soft X-ray radiation results in production of strand breaks as a result of which the supercoiled (sc) form of DNA gets converted to open circular (oc) and linear forms. The disappearance of sc form of DNA can be taken as an index of DNA damage induced by the radiation exposure. Figure 7A shows the agarose gel electrophoresis pattern of plasmid DNA exposed to soft X-ray exposure under different conditions. The control pUC18 DNA contains mostly supercoiled form and only a small amount of the relaxed form (lane 1). Without X-ray exposure, the sample containing 4×10^{-4} mol/dm^3 silybin did not show any effect on the various forms of the DNA, as can be seen from lane 2. When the plasmid DNA is exposed to 10 Gy X-ray radiation, the amount of the sc form decreased due to strand breaks and as a result the intensity of the sc band was reduced (lane 3). However, this radiation induced decrease in the amount of the sc form was prevented by the presence of 4×10^{-4} mol/dm^3 silybin along with the DNA during radiation exposure, as shown in lane 4. This clearly indicates that silybin could offer protection to DNA against radiation induced damage *in vitro* by reducing the formation of strand breaks. Under these experimental conditions, the protection effect should be mainly due to the scavenging of hydroxyl radical by silybin.

Figure 7B shows the percentage (in logarithm) of the remained supercoiled plasmid DNA as a function of dose, in the presence and the absence of silybin. In the applied dose range, both of them show a well linear relationship. Then from the slope, the dose

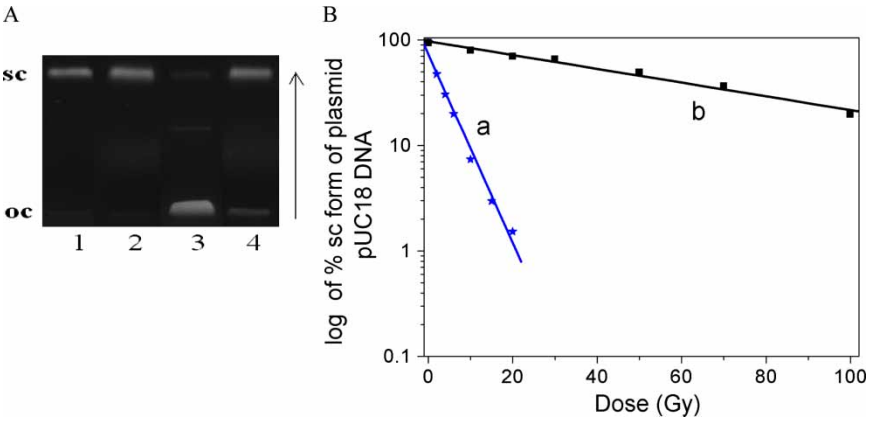

Figure 7. Effect of soft X-ray radiation on plasmid pUC18 DNA in presence and absence of silybin. (A) Agarose gel electrophoresis pattern of plasmid DNA exposed to soft X-ray radiation in presence and absence of silybin. The arrow indicates the running direction of gel. Lane 1: 0 Gy; Lane 2: 0 Gy, 4.0×10^{-4} mol/dm^3 silybin; Lane 3: 10 Gy; Lane 4: 10 Gy, 4.0×10^{-4} mol/dm^3 silybin. (B) Presentation of data as log of % sc form of plasmid pUC18 DNA against various doses of X-ray irradiation.

response parameter D_0 can be calculated: 4.8 Gy for curve a, 86 Gy for curve b as Figure 7B, respectively. Generally, higher D_0 implies better protection effect.

Yield of single strand breakage (G_{SSB})

Figure 8 shows the yield of single-stand breaks in the presence of different concentration of silybin. Six concentrations of silybin were tested, at the 2, 10, 20, 100, 200 and 400×10^{-6} mol/dm^3 level for DNA strand breaks. While the low concentrations (2×10^{-6} mol/dm^3) are at physiological levels, the highest concentration results in the maximum, or near to the maximum, in the reduction of single-strand breaks. As the silybin concentration increased from 0.1 to 4.0×10^{-4} mol/dm^3, the G values for SSB formation decreased from 2.2×10^{-4} to 0.32×10^{-4} μmol/J. At lower silybin concentrations ranging from 2.0×10^{-4} to 4.0×10^{-4} mol/dm^3, the values of SSB yield with silybin concentration changed from (0.45 ± 0.12) to $(0.32 \pm 0.09) \times 10^{-4}$ μmol/J. While at lower concentrations (2.0 and 10.0×10^{-6} mol/dm^3), the values were (5.50 ± 0.46) and $(3.36 \pm 0.28) \times 10^{-4}$ μmol/J, respectively, the variation was much more pronounced than at higher silybin concentrations.

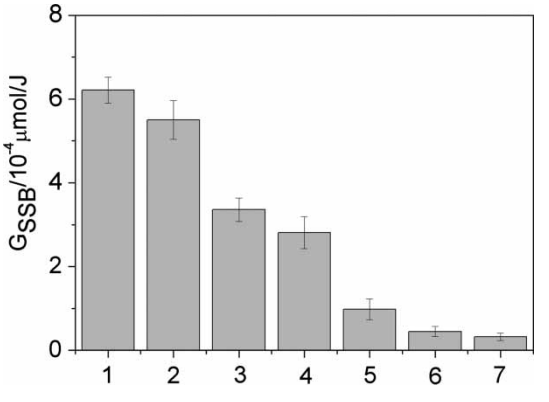

Figure 8. Yields of DNA strand breaks in the presence or the absence of silybin (2–400×10^{-6} mol/dm^3). Error bars present the standard deviation derived from the average of the D_0 values. Lane 1: DNA; Lane 2: DNA-2×10^{-6} mol/dm^3 silybin; Lane 3: DNA-1.0×10^{-5} mol/dm^3 silybin; Lane 4: DNA-2×10^{-5} mol/dm^3 silybin; Lane 5: DNA-1.0×10^{-4} mol/dm^{-3} silybin; Lane 6: DNA-2.0×10^{-4} mol/dm^3 silybin; Lane 7: DNA-4.0×10^{-4} mol/dm^3 silybin.

The significance of our findings awaits definitive studies on the uptake of the different classes of silybin and their distribution in cells. Silybin is uncharged molecule, which should pass through cellular membranes, but it is presently unknown if it can be concentrated inside the cell. Modest binding to DNA has been reported for the flavonol class of flavonoids, e.g. quercetin [40], while it is not known if similar weak binding can occur between silybin and DNA. However, even if there is little increased uptake in cells over the concentrations measures in plasma, our data suggest that silybin can have activity in ameliorating DNA damage at the micromolecular level. Concentrations of antioxidants in the micromolar range cannot compete with cellular constituents, which are present in much higher concentrations for the scavenging of highly reactive ROS species such as OH radicals. Some antioxidants also present the amelioration of free radical damage on DNA by micromolar concentration in the cell. Vitamins C and E in human plasma have been reported as (4.2 ± 1.2) and $(3.1 \pm 0.3) \times 10^{-5}$ mol/dm^3, respectively [41]. Hence, it can be assumed that the protection of DNA at low concentrations could present another biochemical mechanism to counter the consequences of ROS-induced DNA damage. To help understanding this aspect, the investigation by further biological approaches is in progress to elucidate the effect of silybin on X-ray-induced damage in DNA or cells.

Quantum chemical calculations

The relative bond dissociation energies (BDE) were used to evaluate the antioxidant ability. According to

the parameters' definitions, O–H BDE (ΔHOF) = Hr + Hh-Hp, in which Hr is the enthalpy of radical generated through H-abstraction reaction, Hh is the enthalpy of H-atom, −0.49765 hartree, and Hp is the enthalpy of parent molecule. Molecular enthalpy (H) consists of (RO)B3LYP/6-31 G(d)-calculated SPE, AM1-derived thermal contributions to enthalpy (TCE, in which the vibrational contributions including zero point vibrational energy were scaled by a factor of 0.973) [42]. To characterize the O-H BDE, the difference of heat of formation between parent molecule and its free radical (ΔHOF) was employed as a theoretical parameter. The lower the ΔHOF indicates, the weaker the O-H bond, and the more active the antioxidant to scavenge free radicals.

In order to estimate the contribution of hydrogen abstraction mechanism in silybin, the BDEs were calculated for each OH group and are reported in Table II. The sequence of O-H bond dissociation energy in silybin is 4′-OH > 7-OH > 5-OH > 3-OH. The lowest BDE is obtained for the 4′-OH groups (~74 kcal/mol in the gas phase), while the 3-OH BDE is the highest (~101 kcal/mol). These data reveal that the radical at C-4′ is the most stable among all of the positions of phenol ring. The energy difference between this and the next most stable radical (7-OH) was 91.8 kcal/mol, 5-OH to 83.4 kcal/mol, indicating the H-transfer from 5- and 7-OH groups seems to be less effective (high BDE) and 3-OH group does not participate in the H-transfer. This result is in very good agreement with the antioxidant tests of the previous report for flavonoid compounds using (U)B3P86/6-311 + G(d,p) // (U) B3P86/6-31G(d) calculations [39].

It is interesting to compare the experimental structure-activity relationship as well as the theoretical calculations obtained for flavonolignans to those of flavonoids. The recent literature reported BDE calculations at the DFT level on different compounds including quercetin and taxifolin [43,44]. The role of the B-ring has been pointed out, especially in the presence of the catechol moiety (quercetin and taxifolin). The role of the 3-OH group was confirmed in the absence of the 2,3-double bond and the 4′-OH group can easily transfer H to free radicals. Recently, the antioxidant activities of phenols have been correlated with the bond dissociation enthalpy (BDE) of the phenolic O-H bond [45]. Our data of quantum chemical calculations confirmed that the contribution of phenol hydroxyl in ring B appears to be significant. The structure of silybin may lead to enhancement of its antioxidant efficiency due to the presence of an easily abstractable hydrogen atom.

Table II. ΔHOF of the different radical species calculated using DFT B3LYP/6-31G(d,p)/AM1/AM1 method at 298 K.

Radical centre	ΔHOF (kcal/mol)
3-OH	101.1
5-OH	91.8
7-OH	83.4
4′-OH	74.1

Conclusion

Radiation-induced damages to cells and tissues involve generation of reaction oxygen species (ROS) and reactive nitrogen species (RNS) which in turn cause alterations in DNA, membrane-lipids and proteins, eventually leading to cellular dysfunction or cell death [46]. It has been suggested that DNA damage by ROS leads to alteration and elimination of bases, formation of single and double stranded breaks resulting in cell cycle arrest and recruitment of DNA repair enzymes to rescue cells from the DNA damage [47]. The radiation-induced cellular damage may be manifested as clonogenic cell death or alternations in cell-signaling cascades resulting in activation of responsive genes inducing apoptosis.

In the present paper, we have shown that silybin has the antioxidative activity and free radical scavenging properties, which can scavenge various oxidizing radicals such as $^{\bullet}OH$, $Br_2^{\bullet -}$, $N_3^{\bullet}$, $SO_4^{\bullet -}$, $NO_2^{\bullet}$, $CO_3^{\bullet -}$ and $CCl_3OO^{\bullet}$ efficiently. The rate constants of silybin with OH radical (1.8×10^{10} dm^3/mol/s) is diffusion controlled, suggesting that silybin is a potent free radical scavenger. The protection of plasmid DNA from X-ray radiation induced strand breaks by our studies in neutral aqueous media and our recent results [48], the fast chemical reparation of DNA base, further strengthen the potential of this molecule to function as a repair agent and a radioprotector.

Acknowledgements

The authors are grateful to the staff of the Linac Division for their technical assistance in the pulse radiolysis experiments. The authors also thank Dr Kentaro Fujii and Dr Miho Noguchi (Japan Atomic Energy Agency, Japan) for help and discussions during soft X-ray radiation experiments, and Dr Ling Kong (Shangdong University of Technology, China) for help with quantum calculation.

Declaration of interest: The authors report no conflict of interest. The authors alone are responsible for the content and writing of the paper.

References

[1] Kamat JP, Mishra KP. Herbal drugs in radioprotection: modulation by phytochemicals. In: RK Sharma, R Arora, editors. Herbal drug research 21st century prospective. New Delhi: Jaypee; 2006. p 557–567.

[2] Halliwell B, Gutteridge JMC. Free radicals in biology and medicine. Oxford: Oxford Press; 1999.
[3] Winston JC. Health-promoting properties of common herbs. Am J Clin Nutr 1999;70 (Suppl):491–499.
[4] Kren V, Walterova D. Silybin and silymarin–new effects and applications. Biomedicine 2005;149:29–41.
[5] Katiyar SK. Silymarin and skin cancer prevention: anti-inflammatory, antioxidant and immunomodulatory effects (Review). Int J Oncol 2005;26:169–176.
[6] Wellington K, Jarvis B. Silymarin: a review of its clinical properties in the management of hepatic disorders. Biodrugs 2001;15:465–489.
[7] Kvasnicka F, Biba B, Sevcik R, Voldrich M, Kratka J. Analysis of the active components of silymarin. J Chromatogr A 2003; 990:239–245.
[8] Gazak R, Walterova D, Kren V. Silybin and silymarin- new and emerging application in medicine. Curr Med Chem 2007; 14:315–338.
[9] Gyrogy I, Antus S, Foldiak G. Pulse radiolysis of silybin:one-electron oxidation of the flavonoid at neutral pH. Radiat Phys Chem 1992;39:81–84.
[10] Gyorgy I, Antus S, Blazovics A, Foldiak G. Substituent effects in the free radical reactions of silybin: radiation-induced oxidation of the flavonoid at neutral pH. Int J Radiat Biol 1992;61:603–609.
[11] Fu H, Katsumura K, Lin M, Muroya Y. Laser photolysis and pulse radiolysis studies on silybin in ethanol solutions. Radiat Phys Chem 2008;77:1300–1305.
[12] Janata E, Schuler RH. Rate constant for scavenging e_{aq}^- in N_2O saturated solutions. J Phys Chem 1982;86:2078–2084.
[13] Nadezhdin AD, Dunford HB. Horseradish peroxidase.34. Oxidation of compound -II to I by periodate and inorganic anion radicals. Can J Biochem 1979;57:1080–1083.
[14] Monig J, Bahnemann D, Asmus KD. One-electron reduction of carbon tetrachloride in oxygenated aqueous solution: a trichloromethyldioxy radical mediated formation of chloride and carbon dioxide. Chem Biol Interact 1983;47:15–27.
[15] Packer JE, Willson RL, Bahnemann D, Asmus KD. Electron transfer reactions of halogenated peroxyl radicals: measurement of absolute rate constants by pulse radiolysis. J Chem Soc Perkin Trans 1980;2:286–290.
[16] Elliot AJ, Simsons AS. Rate constants for reactions of hydroxyl radicals as a function of temperature. Radiat Phys Chem 1984;24:229–231.
[17] Buxton GV, Stuart CR. Re-evaluation of the thiocyanate dosimeter for pulse radiolysis. J Chem Soc Faraday Trans 1995;91:279–281.
[18] Lin M, Katsumura Y, Hata K, Muroya Y, Nakagawa K. Pulse radiolysis study on free radical scavenger edaravone (3-methyl-1-phenyl-2-pyrazolin-5-one). J Photochem Photobiol B-Biol 2007;89:36–43.
[19] Lewis JG, Stewart W, Adams DO. Role of oxygen radicals in induction of DNA damage by metabolite of benzene. Cancer Res 1988;48:4762–4765.
[20] Mathew D, Nair CKK, Jacob JA, Mukherjee T, Kapoor S, Kagiya TV. Ascorbic acid monoglucoside as antioxidant and radioprotector. J Radiat Res 2007;48:369–376.
[21] Hodgkin PS, Fairman MP, O'Neill P. Rejoining of γ-radiation-induced single-strand breaks in plasmid DNA by human cell extracts: dependence on the concentration of the hydroxyl radical scavenger, tris. Radiat Res 1996;145:24–30.
[22] Spotheim-Maurizot M, Franchet J, Sabattier R, Charlier M. DNA radiolysis by fast neutrons: II. Oxygen, thiols, and ionic strength effects. Int J Radiat Biol 1991;59:1313–1324.
[23] Anderson RF, Fisher LJ, Hara Y, Harris T, Mak WB, Melton LD, Packer JR. Green tea catechins partially protect DNA from OH radical-induced strand breaks and base damage through fast chemical repair of DNA radical. Carcinogenesis 2001;22:1189–1193.
[24] Milligan JR, Aguilera JA, Ward JF. Variation of single-strand break yield with scavenger concentration for plasmid DNA irradiated in aqueous solution. Radiat Res 1993;133:151–157.
[25] Dewar MJS, Zoebisch EG, Healy EF, Stewart JJP. AM1: a new general purpose quantum mechanical molecular model. J Am Chem Soc 1985;107:3902–3909.
[26] Guerra M, Amorati R, Pedulli GF. Water effect on the O-H dissociation enthalpy of para-substituted phenols: a DFT study. J Org Chem 2004;69:5460–5467.
[27] Frisch MJ, Trucks GW, Schlegel HB. Gaussian 03, Revision E.01. Wallingford, CT: Gaussian, Inc.; 2004.
[28] Jovanovic SV, Hara Y, Steeken S, Simic MG. Antioxidant potential of gallocatechins. A pulse radiolysis and laser photolysis study. J Am Chem Soc 1995;117:9881–9888.
[29] Jian L, Wang WF, Zheng ZD, Yao SD, Zhang JS, Lin NY. Reactive intermediates in laser photolysis of guanosine. Res Chem Intermed 1991;15:293–301.
[30] Frank AJ, Gratzel M. Sensitized photoreduction of nitrate in homogeneous and micellar solutions. Inorg Chem 1982;21: 3834–3837.
[31] Huie RE, Clifton CL, Neta P. Electron-transfer reaction-rates and equilibria of the carbonate and sulfate radical-anions. Radiat Phys Chem 1991;38:477–481.
[32] Duthie GG, Wahle KJ. Smoking, antioxidants, essential fatty-acids and coronary heart disease. Biochem Soc Trans 1990; 18:1051–1054.
[33] Richters A. Effects of nitrogen-dioxide and ozone on blood-borne cancer cell colonization of the lungs. J Toxicol Environ Health 1988;25:383–390.
[34] Forni LG, Mora-Arellano VO, Packer JE, Willson RL. Nitrogen dioxide and related free radicals: electron- transfer reactions with organic compounds in solutions containing nitrite or nitrate. J Chem Soc Perkin Trans 2 1986:1–6.
[35] Prutz WA, Monig H, Butler J, Land EJ. Reactions of nitrogen dioxide in aqueous model systems: oxidation of tyrosine units in peptides and proteins. Arch Biochem Biophys 1985; 243:125–134.
[36] Cholbi MR, Paya M, Alcaraz MJ. Inhibitory effects of phenolic compounds on CCl_4- induced microsomal lipid peroxidation. Experientia 1999;47:195–199.
[37] Shen X, Lind J, Eriksen TE, Merenyi G. Reactivity of the $CCl_3OO^\bullet$ radical. Evidence for a first-order transformation. J Phys Chem 1989;93:553–557.
[38] Chevion S, Roberts MA, Chevion M. The use of cyclic voltammetry for the evaluation of antioxidant capacity. Free Radic Biol Med 2000;28:860–870.
[39] DiLabio GA, Pratt DA, LoFaro AD, Wright JS. Theoretical study of X-H bond energetics (X = C, N, O, S): application to substituent effects, gas phase acidities, and redox potentials. J Phys Chem A 1999;103:1653–1661.
[40] Silimani R. Quercetin and DNA in solution: analysis of the dynamics of their interaction with a linear dichroism study. J Biol Macromol 1996;18:287–295.
[41] Lux O, Naidoo D. Biological variation of ascorbic acid and α-tocopherol. Redox Rep 1994;1:45–49.
[42] Trouillas P, Marsal P, Svobodova A, Vostalova J, Gazak R, Hrbac J, Sedmera P, Kren V, Lazzaroni R, Duroux JL, Walterova D. Mechanism of the antioxidant action of silybin and 2,3-dehydrosilybin flavonolignans: a joint experimental and theoretical study. J Phys Chem A 2008;112:1054–1063.
[43] Leopoldini M, Pitarch IP, Russo N, Toscano M. Structure, conformation, and electronic properties of apigenin, luteolin, and taxifolin antioxidants. a first principle theoretical study. J Phys Chem A 2004;108:92–96.
[44] Zhang HY, Sun YM, Wang XL. Substituent effects on OH bond dissociation enthalpies and ionization potentials of catechols: a DFT study and its implications in the rational design of phenolic antioxidants and elucidation of

structure-activity relationships for flavonoid antioxidants. Chem Eur J 2003;9:502–508.
[45] Greenstock CL. Radiation and ageing: free radical damage, biological response and possible antioxidant intervention. Med Hypoth 1993;41:473–482.
[46] Scholes G. Radiation effects on DNA. The silvanous Thomson Memorial Lecture. Br J Radiol 1982;56:221–231.
[47] Wright JS, Johnson ER, Dilabio GA. Predicting the activity of phenolic antioxidants: theoretical method, analysis of substituent effects, and application to major families of antioxidations. J Am Chem Soc 2001;123:1173–1183.
[48] Fu H, Katsumura Y, Lin M, Hata K, Muroya Y, Hatano Y. Fast repair activities towards dGMP hydroxyl radical adducts by silybin and its analogues. J Radiat Res 2008;49:609–614.

This paper was first published online on iFirst on 11 August 2009.